

# 3D Surface Realignment Tracking for Medical Imaging: A Phantom Study with PET Motion Correction

Oline V. Olesen, Rasmus R. Paulsen, Rasmus R. Jensen, Sune H. Keller,  
Merence Sibomana, Liselotte Højgaard, Bjarne Roed, and Rasmus Larsen

**Abstract** We present a complete system for motion correction in high resolution brain positron emission tomography (PET) imaging. The system is based on a compact structured light scanner mounted above the patient tunnel of the Siemens High Resolution Research Tomograph (HRRT) PET brain scanner. The structured light system is equipped with a near infrared diode and uses phase-shift interferometry (PSI) to compute 3D point clouds of the forehead of the patient. These 3D point clouds are progressively aligned to a reference surface, thereby giving the head pose changes. The estimated pose changes are used to reposition a sequence of reconstructed PET frames. To align the structured light system with the PET coordinate system, a novel registration algorithm based on the PET transmission scan and an initial surface has been developed. The performance of the complete setup has been evaluated using a custom-made phantom, based on a plastic mannequin head equipped with two positron-emitting line sources. Two experiments were performed. The first simulates rapid and short head movements, while the second simulates slow and continuous movements. In both cases, the system was able to produce PET scans with focused PET reconstructions. The system is nearly ready for clinical testing.

---

O.V. Olesen (✉) · R.R. Paulsen · R.R. Jensen · R. Larsen  
Informatics and Mathematical Modelling, Technical University of Denmark, Richard Petersens  
Plads, Building 321, 2800 Kgs. Lyngby, Denmark  
e-mail: [ovol@imm.dtu.dk](mailto:ovol@imm.dtu.dk)  
url: <http://www.imm.dtu.dk/>

O.V. Olesen · S.H. Keller · M. Sibomana · L. Højgaard  
Department of Clinical Physiology, Nuclear Medicine & PET, Rigshospitalet, Copenhagen  
University Hospital, University of Copenhagen, Blegdamsvej 9, 2100 Copenhagen, Denmark

O.V. Olesen · B. Roed  
Siemens Healthcare, Siemens A/S, Borupvang 3, 2750 Ballerup, Denmark

Y.(J.) Zhang (ed.), *Image-Based Geometric Modeling and Mesh Generation*,  
Lecture Notes in Computational Vision and Biomechanics 3,  
DOI [10.1007/978-94-007-4255-0\\_2](https://doi.org/10.1007/978-94-007-4255-0_2), © Springer Science+Business Media Dordrecht 2013

## 1 Introduction

Patient head movement during high resolution brain positron emission tomography (PET) scanning will cause blurring and ghosting [3]. The low count rate and resulting low contrast makes it almost impossible to perform motion correction on raw PET data, and therefore most methods rely on external tracking of the head movement [10–12, 16]. The Polaris Vicra (Northern Digital Inc.) tracking system has been used as the reference on many PET installations [6]. While the Polaris system is well tested and accurate, it suffers from problems related to attaching optical markers to the patient’s head. Experience shows that in a clinical setting, the markers are difficult to attach such that they stay in position during the entire scan. A markerless system that fits into the narrow PET tunnel will improve the clinical acceptance and the diagnostic value of PET brain scans.

We have previously described a structured light based system that is based on a small projector and two small cameras [7] for tracking patient head pose. This system has been modified as described below and it is referred to as Tracoline. The Tracoline system has been designed to fit into the patient tunnel of the Siemens High Resolution Research Tomograph (HRRT) PET brain scanner. The HRRT PET scanner has a spatial resolution down to 1.4 mm [8] and is therefore well suited for testing new motion correction methods. The Tracoline system is based on the progressive reconstruction of 3D surfaces of the upper face region of the patient in the scanner. The pose changes are found by computing the rigid transformation between the current scan and the initial surface scan. The system described in [7] was based on visible light and did not operate in real time. Visible light scanners are not suited for repeated human facial scans. Furthermore, to be functional the system needs to acquire frames sufficiently fast to faithfully capture patient head movements. In this paper, we describe a system using invisible light with a camera acquisition rate of 30 frames per second.

While the previous paper focused on measuring the accuracy of the structured light tracking system using a rotation stage as ground truth [7], the real interest is the improvement of the PET scans. To be able to evaluate the quality improvement of the PET scan, a scan using a radioactive tracer must be performed. A common approach is to use a phantom and compare the resulting PET scan with the known geometry of the phantom [8]. We have therefore designed a customized phantom with a radioactive source and used this in the evaluation of the Tracoline based motion correction. Our system setup with the Tracoline system and the custom phantom can be seen in Fig. 1. Compared to other external tracking systems, where the geometric alignment between the tracking system and the PET scanner can be problematic, we investigate a novel alignment approach based on aligning the Tracoline system scan directly to the PET transmission scan.

## 2 Experiments and Methods

The Tracoline system consists of two Point Grey Flea2 cameras ( $1288 \times 964$  pixels), each running at 30 frames per second. The Pico Digital Light Processing (DLP) pro-

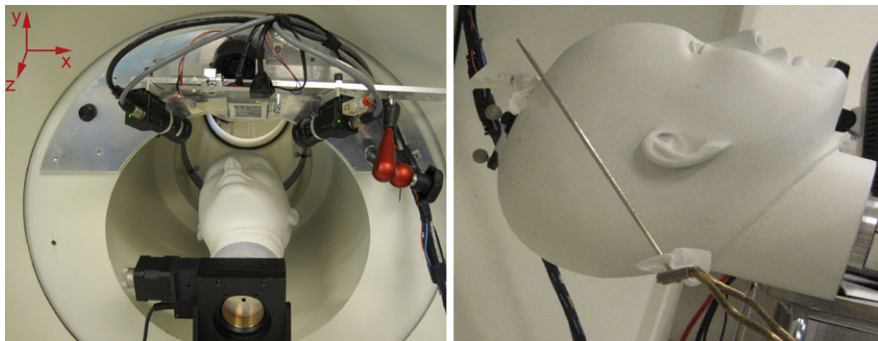


**Fig. 1** *Left:* The patient tunnel of the HRRT PET scanner with the Tracoline system mounted. The phantom is mounted on a rotating stage rotated to the right ( $-10$  degrees). *Right:* The phantom including one of the two radioactive line sources. It is placed in the head in the same angle as shown here to simulate the brain

jector from Texas Instruments is used to project phase-modulated patterns. One of the light diodes of the Pico projector has been replaced with a near infrared (NIR) diode resulting in a non-visible projected pattern. The projector is controlled by a GFM Pico developer kit board that also sends trigger pulses to the cameras, in order to synchronize the projected patterns and the shutter of the cameras. A multi-threaded C++ program running on a standard portable computer acquires the real time camera data and stores them as image files. The 3D point cloud generation, surface reconstruction, and alignment are done in a post-processing step. The Tracoline system and HRRT PET acquisition computer are synchronized through an internal network time protocol (NTP) server.

The 3D point cloud generation is based on phase-shifting interferometry (PSI) [5] where a set of 2D interferograms are projected and projector-camera correspondence can be found using phase unwrapping. This is explained in detail in [5, 7]. While three patterns are used in [7], the system is now extended to use six patterns with varying wavelengths to make the phase unwrapping more robust to discontinuities in the surface. Since each point cloud computation requires six frames, the effective tracking frequency is 5 Hz. A surface is reconstructed using a modern algorithm [9] based on the point cloud acquired in the initial position. The facial pose changes are then found by rigidly aligning the following surface scans to this reference surface using an optimized, iterative, closest point (ICP) algorithm [15].

To correct for motion, we need to know the transformation between the HRRT PET scanner coordinate system and the Tracoline system. To estimate this transformation, we use the transmission scan of the HRRT PET scanner, which is also used for the attenuation and scatter correction within normal PET reconstruction. The transmission scan is a voxel volume similar to a computed tomography (CT) scan. The initial reference surface scan is captured by the Tracoline system during the transmission scan, thus creating correspondence. The transformation is computed using a pseudo-ICP algorithm [13]. The surface scan is scaled to fit the volume, and manually rotated and translated into an initial position. To find correspondence

between surface sample points and the volume, the volume is sampled in the normal direction (both positive and negative) of the surface scan to find the point with maximum gradient. Knowing the general orientation of the patient in the PET scanner, we use the absolute gradient in the x (left/right) and z (axial) direction and the negative gradient for the y (anterior/posterior) direction:

$$\Delta f = \left| \frac{\partial f}{\partial x} \right| - \frac{\partial f}{\partial y} + \left| \frac{\partial f}{\partial z} \right|$$

With a point correspondence, a rigid transformation is found using the closed-form loop to estimate the absolute transformation [4]. With an initialization, transformation, this process is iterated until the transformation of the Tracoline scan converges to the volume data.

In order to apply the motion correction to the PET data, we apply the multiple acquisition frames (MAF) method [10]. In [8] the MAF method was demonstrated on the Siemens HRRT PET scanner using the tracking input from the Polaris Vicra system. We divide the PET emission list mode data into equal time length intervals and, for each interval, a PET frame is reconstructed using the 3D ordered subset expectation maximization (3D-OSEM) algorithm with resolution modeling and incorporating a spatially invariant point spread function [14]. These frames are then repositioned to a reference position using the Tracoline tracking system.

A custom phantom with known geometry was designed. It consists of a hollow plastic mannequin head with a very low attenuation coefficient. Two radioactive line sources are inserted into the head to provide activity for the HRRT PET scanner. The activities of the line sources are  $2 \times 7.8$  MBq each, created by a positron-emitting germanium-68/gallium-68 generator. As can be seen in Fig. 1, the line sources go through the head from the back of the skull to the forehead. The phantom was mounted onto a rotation stage by Thorlabs and placed in the patient tunnel of the HRRT PET scanner.

Two experiments were performed using the stage to rotate the head. In experiment one, the head was rotated from  $-20$  to  $20$  degrees in steps of  $5$  degrees. At each position a  $30$  s frame was PET reconstructed and repositioned. Data with motion was excluded from the reconstruction. In experiment two, the head was rotated from  $-10$  to  $10$  degrees in a continuous motion with a maximum speed of one degree per second. The PET data was reconstructed using one second frames in experiment two. Experiment one simulates the clinical situation where the patient is performing a rapid head motion followed by a stationary period. State of the art practice is to discard PET data during such rapid motions. The second experiment simulates e.g. a patient falling asleep, where the head is slowly drifting from side to side.

We evaluate the effect of the motion correction on the reconstructed PET images by calculating Dice's coefficient (percent volume overlap) [1] between a reference image recorded without phantom motion, the motion distorted image, and the Tracoline based motion-corrected image. The number of voxels,  $N$ , included in the calculation is set to a value corresponding to the number of voxels inside the tubes  $2.5$  times the diameter of the PET sources used (outer diameter  $3.2$  mm and active

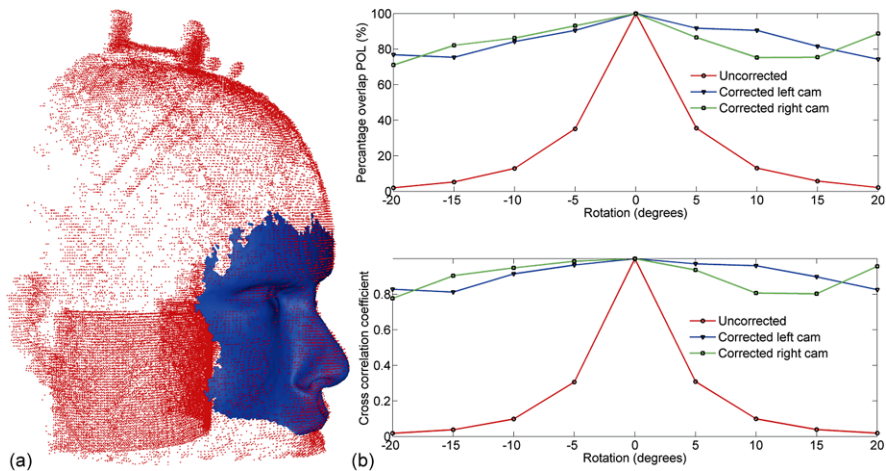


**Fig. 2** (a) shows the alignment between maximum gradient points in the transmission scan shown as *red dots* and the Tracoline face scan shown as a *blue surface*. (b) shows quantitative results of the stepwise experiment. *Top*: the percentage of overlapping points in the reference PET image compared to the unaligned/aligned PET images based on either the right or the left camera. *Bottom*: the cross correlation between the reference PET image and the unaligned/aligned PET images

length 168 mm) [8]. The extended volume is used in order to compensate for partial volume effects. In each image to be studied, the set of the  $N$  most intense voxels is extracted and used for the Dice's coefficient computation, presented as the percentage of overlapping voxels. In addition we compute the normalized cross correlation between the reference image and each image frame, either motion-corrected or uncorrected [2].

### 3 Results and Discussion

The rigid transformation between the coordinate system of the Tracoline system and the PET image frame is obtained from using the described surface-to-volume alignment. Figure 2(a) shows the reference surface aligned to maximum gradient points in the transmission scan.

Figure 2(b) shows the results of the first experiment with stepwise rotation of the phantom. The top figure shows the percentage overlap between PET frames of the line sources in the reference position and a scan position as a function of the performed rotation of the head. Similarly, the bottom plot of Fig. 2(b) shows the correlation coefficient between the reference image and a motion-corrected/uncorrected image for the different scan positions. Results based on tracking information from the left and right camera of the Tracoline system are shown in green and blue colors respectively, while the red curve represents the uncorrected image results. The overlap and the correlation measures are in agreement. The results of the uncorrected frames decrease with the size of performed rotation from an overlap of 100%

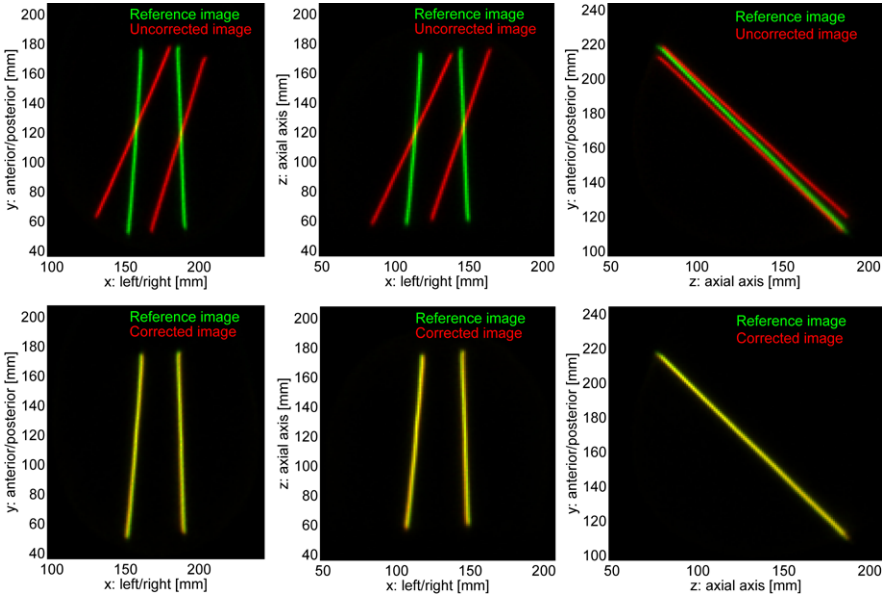


**Fig. 3** The figure shows the summation of the PET images along 3 different axes for a reference image (shown in *green*) and a target image (shown in *red*) with a 20 degree rotation (overlap = 89%, shown in *yellow*). The uncorrected image is shown as captured in the *first row*, while the second row shows the image after motion correction

down to 2% at  $\pm 20$  degrees. The overlap of the motion-corrected reconstruction is improved significantly for all positions with percentage overlap of 71–93%. The overlap is not 100%, which is mainly due to the internal calibration of the Tracoline system, the ICP alignment, and the geometrical alignment with the HRRT PET scanner. In addition, the interpolation error, combined with the straight and narrow line sources of the phantom (with a diameter similar to the voxel size of 1.2 mm), induces partial volume effects and thereby decreases the overlap and correlation measure. The differences between the left camera and the right camera could be explained by the construction of the reference surface scan, where left camera was chosen as the basis. The result is similar to [8], where the overlap was 65–85% for a 10 degrees corrected rotation. However, the two studies cannot be directly compared since the phantom designs are different.

A visual evaluation of the motion correction is shown in Fig. 3 for the maximum rotation of 20 degrees. The PET images are summed along one dimension and visualized on top of each other pairwise in the red and green color channels. The overlapping pixels of the two PET images appear yellow. The top row of the figure shows the reference image and the uncorrected image as two sets of rods rotated approximately 2 cm at the end points. These correspond to the relevant brain regions: the frontal lobe and cerebellum. The bottom row shows the reference image and the corrected image seen as two yellow rods, demonstrating a near-perfect mo-

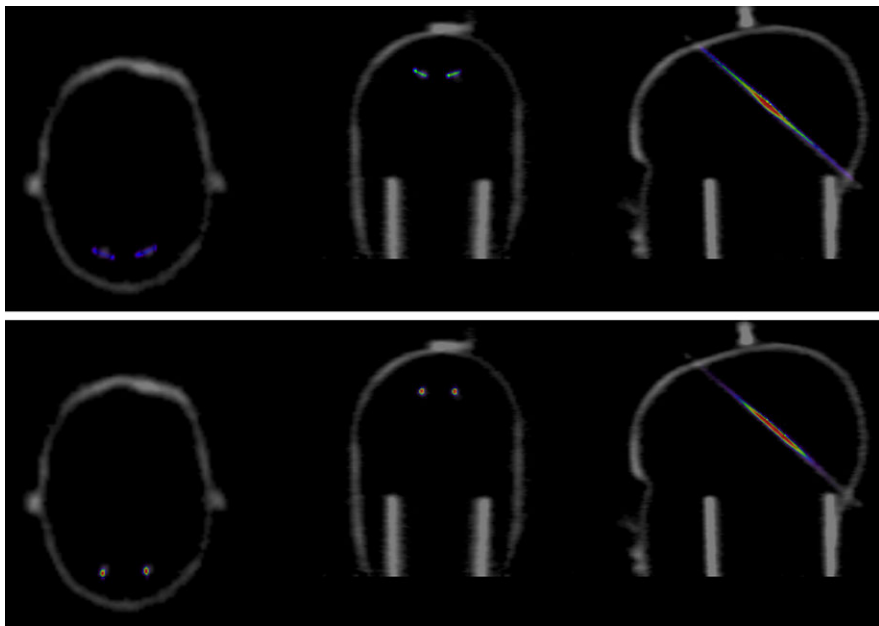


**Fig. 4** Results of the dynamic PET scan. One-hundred, one-second frames uncorrected (*top*) and MAF motion corrected (*bottom*) are summed and fused with a transmission scan. The frame repositioning is based on the left camera alignment

tion correction. This position has an overlap of 89% in contrast to the rotation of  $-20$  degrees with an overlap of 71%.

The results of the second experiment, with a continuous rotation of 20 degrees demonstrating the realtime pose registration of the Tracoline system, are presented in Fig. 4. The one second PET frames are summed and fused with the transmission image of the phantom. The top of the figure shows a row of uncorrected images, where the motion of the line sources is seen as blurred circle parts. The bottom row shows the motion-corrected image, where the previously blurred parts appear in focus and with high intensity. The cross section of the line sources shows dots with a diameter of only a few pixels. Long drift motion is a very complex problem to overcome using image registration methods for motion estimation, and this is why an external tracking system is of great value. Our latest results show that continuous motion can be tracked in real time and PET frames successfully corrected.

## 4 Summary and Conclusions

This paper describes a complete system for motion correction in high resolution PET brain imaging. It is based on a small and flexible structured light scanner mounted above the patient tunnel of the PET scanner. The scanner is equipped with a near infrared light source, making it suitable for future patient examinations. Furthermore,

the system tracks the head pose changes with a frequency of 5 Hz, which is suitable for the head movement experienced during real clinical PET scanning. In order to align the two systems, a novel algorithm using the HRRT PET transmission scan and the initial surface scan was presented. The performance of the system was evaluated using a custom-designed phantom with two radioactive line sources mounted on a programmable rotation stage. The results of the two experiments are very promising. The first experiment simulates rapid but short head movements and the second experiment simulates slow but longer head movements. Quantitative analysis shows that the combined system is able to robustly reduce motion artifacts and greatly improve PET scans for scenarios involving both slow and rapid movements. The system is nearly ready for actual clinical testing.

**Acknowledgements** The John and Birthe Meyer Foundation is thanked for the generous donation of the HRRT PET scanner and the cyclotrons for isotope production.

## References

1. Dice LR (1945) Measures of the amount of ecologic association between species. *Ecology* 26(3):297–302
2. Gonzalez RC, Woods RE (2002) Digital image processing. Prentice Hall, New York
3. Green MV, Seidel J, Stein SD, Tedder TE, Kempner KM, Kertzman C, Zeffiro TA (1994) Head movement in normal subjects during simulated PET brain imaging with and without head restraint. *J Nucl Med* 35(9):1538–1546
4. Horn BKP (1987) Closed form solution of absolute orientation using unit quaternions. *J Opt Soc Am A* 4(4):629–642
5. Huang PS, Hu Q, Jin F, Chiang FP (1999) Color-encoded digital fringe projection technique for high-speed three-dimensional surface contouring. *Opt Eng* 38(6):1065–1071
6. Lopresti BJ, Russo A, Jones WF, Fisher T, Crouch DG, Altenburger DE, Townsend DW (1999) Implementation and performance of an optical motion tracking system for high resolution brain PET imaging. *IEEE Trans Nucl Sci* 46(6):2059–2067
7. Olesen OV, Paulsen RR, Højgaard L, Roed B, Larsen R (2010) Motion tracking in narrow spaces: a structured light approach. *Lect Notes Comput Sci* 6363:253–260
8. Olesen OV, Svarer C, Sibomana M, Keller SH, Holm S, Jensen JA, Andersen F, Højgaard L (2010) A movable phantom design for quantitative evaluation of motion correction studies on high resolution PET scanners. *IEEE Trans Nucl Sci* 57(3):1116–1124
9. Paulsen RR, Bærentzen JA, Larsen R (2010) Markov random field surface reconstruction. *IEEE Trans Vis Comput Graph* 16:636–646
10. Picard Y, Thompson CJ (1997) Motion correction of PET images using multiple acquisition frames. *IEEE Trans Med Imaging* 16(2):137–144
11. Raghunath N, Faber TL, Suryanarayanan S, Votaw JR (2009) Motion correction of PET brain images through deconvolution: II. Practical implementation and algorithm optimization. *Phys Med Biol* 54(3):813
12. Rahmim A, Dinelle K, Cheng JC, Shilov MA, Segars WP, Lidstone SC, Blinder S, Rousset OG, Vajihollahi H, Tsui B, Wong DF, Sossi V (2008) Accurate event-driven motion compensation in high-resolution PET incorporating scattered and random events. *IEEE Trans Med Imaging* 27(8):1018–1033
13. Rusinkiewicz S, Levoy M (2001) Efficient variants of the ICP algorithm. In: *Proc. third international conference on 3-D digital imaging and modeling*, pp 145–152



14. Sureau FC, Reader AJ, Comtat C, Leroy C, Ribeiro MJ, Buvat I, Trébossen R (2008) Impact of image-space resolution modeling for studies with the high-resolution research tomograph. *J Nucl Med* 49(6):1000
15. Wilm J, Olesen O, Paulsen R, Højgaard L, Roed B, Larsen R (2011) Real time surface registration for PET motion tracking. *Lect Notes Comput Sci* 6688:166–175
16. Woo S-K, Watabe H, Choi Y, Kim KM, Park CC, Bloomfield PM, Iida H (2004) Sinogram-based motion correction of PET images using optical motion tracking system and list-mode data acquisition. *IEEE Trans Nucl Sci* 51(3):782–788



<http://www.springer.com/978-94-007-4254-3>

Image-Based Geometric Modeling and Mesh Generation

Zhang, Y.J. (Ed.)

2013, XI, 301 p., Hardcover

ISBN: 978-94-007-4254-3